Tomáš Vejchodský; Radek Erban
Deterministic and stochastic models of dynamics of chemical systems

In: Jan Chleboun and Petr Přikryl and Karel Segeth and Tomáš Vejchodský (eds.): Programs and Algorithms of Numerical Mathematics, Proceedings of Seminar. Dolní Maxov, June 1-6, 2008. Institute of Mathematics AS CR, Prague, 2008. pp. 220–225.

Persistent URL: http://dml.cz/dmlcz/702876

DETERMINISTIC AND STOCHASTIC MODELS OF DYNAMICS OF CHEMICAL SYSTEMS*

Tomáš Vejchodský, Radek Erban

1. Introduction

The deterministic and stochastic models are two principal approaches for modeling of the dynamics of the chemical reactions. The deterministic models are usually based on differential equations for concentrations (or amounts of molecules) of particular chemical species whereas the *stochastic simulation algorithms* (SSA) use the pseudorandom number generators. Of course, different realizations of the SSA differ from each other, but a mean value over many realizations is a well reproducible quantity which describes the average behavior of the system.

In this paper, we examine an example motivated by chemical processes in living cells. In this example, we observe qualitatively different behaviors of the deterministic and stochastic models. Namely, the solution of the deterministic model converges to a stationary state while the stochastic solution exhibits an oscillatory character. This discrepancy is caused by the fact that the deterministic model is inexact if the number of molecules of a chemical species is too small. In this case, the more accurate stochastic model should be used. However, the disadvantage of the stochastic approach lies in its high computational cost. We show that certain quantities obtained from the SSA can be computed as solutions of deterministic partial differential equations which is much less computationally intensive.

2. Chemical system with SNIPER bifurcation

The chemical processes in cells often exhibit *saddle-node infinite period* (SNIPER) bifurcation, see for example the model of the cell cycle regulation [3]. The following simple system of seven chemical reactions exhibits the same behavior. We consider two chemical species X and Y in a well-mixed reactor of volume V which are subject to the following reactions

$$\emptyset \xrightarrow{k_{1d}} Y \xrightarrow{k_{2d}} X \xrightarrow{k_{3d}} \emptyset \qquad 2X \underset{k_{5d}}{\overset{k_{4d}}{\rightleftarrows}} 3X \tag{1}$$

$$X + Y \xrightarrow{k_{6d}} X + 2Y \qquad 2X + Y \xrightarrow{k_{7d}} 2X. \tag{2}$$

*This work has been supported by grants No. 102/07/0496 of the Czech Science Foundation, No. IAA100760702 of the Grant Agency of the Academy of Sciences and by the institutional research plan No. AV0Z10190503 of the Academy of Sciences of the Czech Republic.

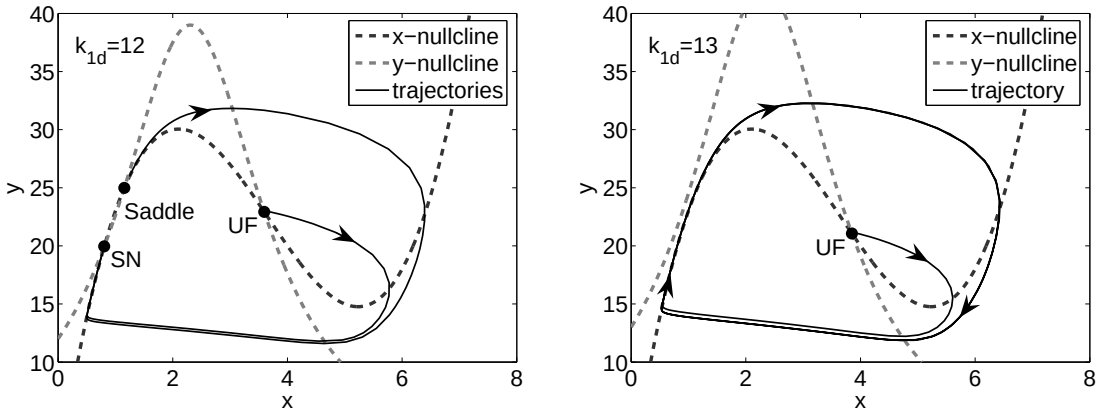

Fig. 1: *Nullclines of the ODE system* (3) *for* $k_{1d} = 12$ *(left) and* $k_{1d} = 13$ *(right). The other parameter values are given by* (4)*. The steady states are denoted by dots. Illustrative trajectories which start close to the steady states are plotted as thin black lines. The stable direction of the saddle is indicated by the dashed line.*

Here $k_{1d}, \ldots, k_{7d}$ are the so-called rate constants which describe the speed of the reactions. The symbol $\emptyset$ denotes the chemical species of no interest. Hence, for example the first reaction is the production of Y from the source with the rate constant k_{1d}.

Let $X = X(t)$ and $Y = Y(t)$ stand for the number of molecules of the two chemical species. If the numbers X and Y are sufficiently high then the dynamics of the system (1)–(2) can be described by the mean-field ODE model

$$\frac{\mathrm{d}\widetilde{x}}{\mathrm{d}t} = k_{2d}\,\widetilde{y} - k_{5d}\,\widetilde{x}^3 + k_{4d}\,\widetilde{x}^2 - k_{3d}\,\widetilde{x}, \quad \frac{\mathrm{d}\widetilde{y}}{\mathrm{d}t} = -k_{7d}\,\widetilde{x}^2\,\widetilde{y} + k_{6d}\,\widetilde{x}\,\widetilde{y} - k_{2d}\,\widetilde{y} + k_{1d}, \quad (3)$$

where $\widetilde{x} = X/V$ and $\widetilde{y} = Y/V$ stand for the concentrations of X and Y, respectively. We choose the values of the rate constants as

$$k_{1d} = 12\ [\mathrm{sec}^{-1}\mathrm{mm}^{-3}], \quad k_{2d} = 1\ [\mathrm{sec}^{-1}], \quad k_{3d} = 33\ [\mathrm{sec}^{-1}], \quad k_{4d} = 11\ [\mathrm{sec}^{-1}\mathrm{mm}^{3}],$$
$$k_{5d} = 1\ [\mathrm{sec}^{-1}\mathrm{mm}^{6}], \quad k_{6d} = 0.6\ [\mathrm{sec}^{-1}\mathrm{mm}^{3}], \quad k_{7d} = 0.13\ [\mathrm{sec}^{-1}\mathrm{mm}^{6}]. \quad (4)$$

In this case the nullclines $\mathrm{d}\widetilde{x}/\mathrm{d}t = 0$ and $\mathrm{d}\widetilde{y}/\mathrm{d}t = 0$ intersect at three steady states denoted by SN (stable node), Saddle, and UF (unstable focus), see Figure 1 (left), where also illustrative trajectories are shown. We observe that the system converges to the steady state at the SN. However, if we change the bifurcation parameter k_{1d} to have the value 13, we observe the behavior shown in Figure 1 (right). The system possesses a periodic solution.

The SN and the Saddle lie on the invariant cycle, which is a union of these two steady states and two heteroclinic trajectories connecting these steady states. While increasing the value of k_{1d}, the SN and the Saddle collaps into a single steady state which disappears if we increase the value of k_{1d} over a critical value $K_d \doteq 12.2$. This is known as the SNIPER bifurcation.

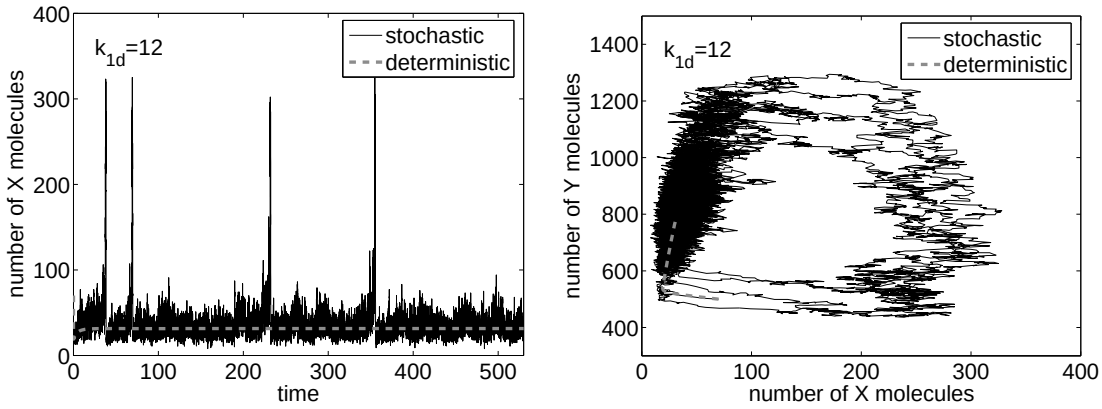

Fig. 2: *Trajectories of the deterministic and stochastic models for* $k_{1d} = 12$.

In Figure 2 we may compare the trajectories of the deterministic model (3) and the stochastic model for the parameter values given by (4). Notice the convergence of the deterministic solution to the steady sate and the oscillatory behavior of the stochastic solution. On the other hand if we change the bifurcation parameter to $k_{1d} = 13$ then both deterministic and stochastic models oscillate.

3. Gillespie stochastic simulation algorithm

The stochastic trajectories in Figures 2 were obtained by the Gillespie SSA [2]. To describe this algorithm we define the following propensity functions

$$\alpha_1(x,y) = k_1, \quad \alpha_2(x,y) = k_2 y, \quad \alpha_3(x,y) = k_3 x, \quad \alpha_4(x,y) = k_4 x(x-1),$$
$$\alpha_5(x,y) = k_5 x(x-1)(x-2), \quad \alpha_6(x,y) = k_6 xy, \quad \alpha_7(x,y) = k_7 x(x-1)y, \quad (5)$$

where $k_1 = k_{1d}V,\ k_2 = k_{2d},\ k_3 = k_{3d},\ k_4 = k_{4d}/V,\ k_5 = k_{5d}/V^2,\ k_6 = k_{6d}/V,\ k_7 = k_{7d}/V^2$ are the scaled rate constants. The Gillespie SSA follows these steps.

1. Generate two random numbers r_1, r_2 uniformly distributed in $(0,1)$.
2. Compute the cumulative propensity function $\alpha_0(t) = \sum_{i=1}^{7} \alpha_i(X(t), Y(t))$.
3. Compute the time interval to the next reaction $\tau = \dfrac{1}{\alpha_0(t)} \ln\left(\dfrac{1}{r_1}\right)$.
4. At time $t + \tau$ the j-th reaction takes place. Determine j by

$$\frac{1}{\alpha_0(t)} \sum_{i=1}^{j-1} \alpha_i(X(t), Y(t)) \le r_2 < \frac{1}{\alpha_0(t)} \sum_{i=1}^{j} \alpha_i(X(t), Y(t)).$$

5. Update the numbers of reactants and products according to the j-th reaction.
6. Put $t := t + \tau$ and go to 1.

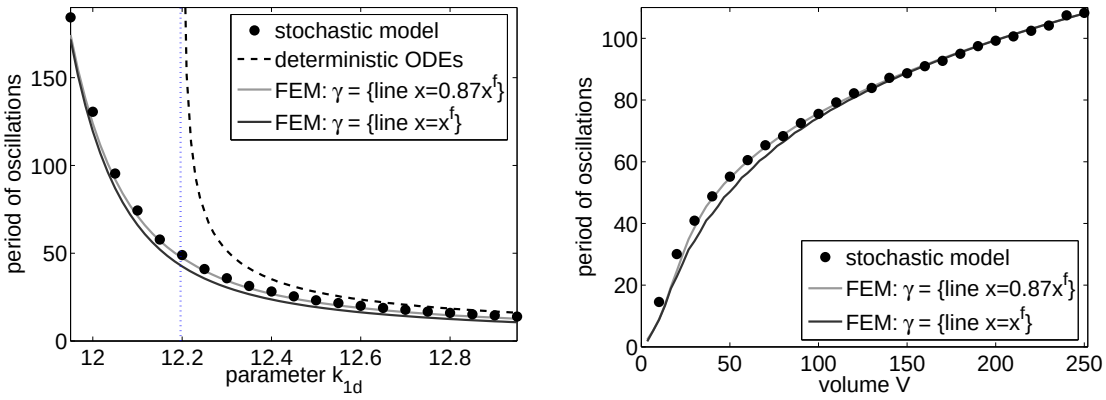

Fig. 3: *The mean period of oscillations of the deterministic (dashed line, see [1] for details) and stochastic (points) models as a function of k_{1d} for $V = 40$ (left) and as a function of V for the bifurcation value $k_{1d} = K_d \doteq 12.2$ (right). Two estimates computed by formula* (12) *with different γ are indicated by gray lines.*

4. Period of oscillations

An important characteristic of the chemical system (1)–(2) is the mean period of its oscillations. This period is shown in Figure 3 for both deterministic and stochastic models. The periods for the stochastic model are computed as an average over 10 000 realizations which is computationally intensive. Here, we show that these values can be obtained by solving and analyzing the chemical Fokker-Planck equation.

The stationary chemical Fokker-Planck equation for the stationary distribution P_s, see [1] for more details, can be formulated in the following way

$$-\operatorname{div}(\mathcal{A}\nabla P_s + P_s\mathbf{b}) = 0, \tag{6}$$

where $\mathcal{A} = -\begin{pmatrix} d_x & d_{xy}/2 \\ d_{xy}/2 & d_y \end{pmatrix}$, $\mathbf{b} = \left(v_x - \dfrac{\partial d_x}{\partial x} - \dfrac{1}{2}\dfrac{\partial d_{xy}}{\partial y}, v_y - \dfrac{\partial d_y}{\partial y} - \dfrac{1}{2}\dfrac{\partial d_{xy}}{\partial x}\right)$, and $v_x = \alpha_2 - \alpha_3 + \alpha_4 - \alpha_5$, $v_y = \alpha_1 - \alpha_2 + \alpha_6 - \alpha_7$, $d_x = [\alpha_2 + \alpha_3 + \alpha_4 + \alpha_5]/2$, $d_y = [\alpha_1 + \alpha_2 + \alpha_6 + \alpha_7]/2$, $d_{xy} = -\alpha_2$.

The stationary distribution $P_s = P_s(x, y)$ is normalized to satisfy

$$\int_0^\infty \int_0^\infty P_s(x, y)\,\mathrm{d}x\mathrm{d}y = 1, \qquad P_s(x, y) \geq 0, \qquad (x, y) \in [0, \infty) \times [0, \infty). \tag{7}$$

Here, $P_s(x, y)$ is the probability that $X(t) \to x$ and $Y(t) \to y$ as $t \to \infty$. To find numerically the stationary distribution P_s for system (1)–(2) with parameter values (4) we truncate the infinite domain $(0, \infty) \times (0, \infty)$ to $S = (0, 500) \times (0, 2000)$, denote by $\mathbf{n}$ is the unit outward normal vector to ∂S and prescribe the boundary conditions

$$(\mathcal{A}\nabla P_s + P_s\mathbf{b}) \cdot \mathbf{n} = 0 \quad \text{on } \partial S. \tag{8}$$

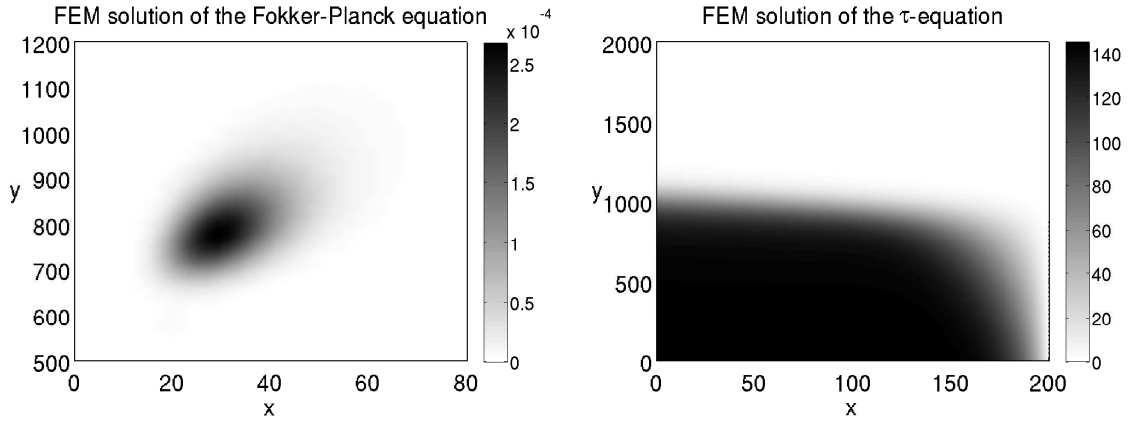

Fig. 4: *The stationary distribution $P_{s,h}$ (left) and the mean exit time τ_h (right).*

The finite element solution $P_{s,h}$ to problem (6)–(8) is derived in a standard way and it is determined by the requirements $P_{s,h} \in W_h$ and

$$\int_S \big(\mathcal{A}\nabla P_{s,h} + P_{s,h}\mathbf{b}\big) \cdot \nabla\varphi_h \,\mathrm{d}x\mathrm{d}y = 0 \quad \forall\varphi_h \in W_h,$$

where W_h is a suitable finite dimensional subspace of the Sobolev space $H^1(S)$. In our case W_h consists of continuous and piecewise linear functions over a triangulation of S. The finite element solution $P_{s,h}$ is provided in Figure 4 (left). Alternatively, the stationary distribution can be obtained by computationally very intensive long time stochastic simulations. However, the numerical solution of (6)–(8) is much faster and equally accurate as the stochastic simulations.

Let us point out that equation (6) with boundary condition (8) possesses a trivial solution $P_s = 0$ but we are interested in a nontrivial one. We obtain the nontrivial approximation $P_{s,h}$ by a standard software for computation of eigenvectors corresponding to the zero eigenvalue of a sparse matrix. The resulting solution is then normalized to satisfy (7) with the integrals taken over S.

The stationary distribution, see Figure 4 (left), shows that the system spends most of the time in the strip $X < 200$. Observing Figure 2 we may say that an oscillation occurs if $X > 200$. The stationary distribution P_s is almost zero for $x > 200$ and therefore, it is very unlikely to find the system in a state with $X > 200$. Thus, we neglect the time the system spends in the halfplane $X > 200$ and approximate the mean period of oscillations as the average time to leave the domain $X < 200$ provided the system just entered it.

To this end, we define the subdomain $\widetilde{S} = (0, 200) \times (0, 2000)$ of S and formulate the adjoint equation to (6) with suitable boundary conditions

$$-\operatorname{div}(\mathcal{A}\nabla\tau) + \mathbf{b} \cdot \nabla\tau = -1 \quad \text{in } \widetilde{S}, \tag{9}$$

$$\tau = 0 \quad \text{on the line } x = 200, \tag{10}$$

$$(\mathcal{A}\nabla\tau) \cdot \mathbf{n} = 0 \quad \text{on lines } y = 0,\ y = 2000,\ x = 0. \tag{11}$$

The quantity $\tau = \tau(x, y)$ is known [1] to model the average time to leave $\widetilde{S}$ provided the system is in the state $X(t) = x$ and $Y(t) = y$. The finite element approximation $\tau_h \in \widetilde{W}_h$ of τ is uniquely determined by the identity

$$\int_{\widetilde{S}} (\mathcal{A}\nabla\tau_h) \cdot \nabla\varphi_h \,\mathrm{d}x\mathrm{d}y + \int_{\widetilde{S}} \mathbf{b} \cdot \nabla\tau_h \,\varphi_h \,\mathrm{d}x\mathrm{d}y = \int_{\widetilde{S}} -1 \cdot \varphi_h \,\mathrm{d}x\mathrm{d}y \quad \forall\varphi_h \in \widetilde{W}_h,$$

where $\widetilde{W}_h$ is a space of continuous and piecewise linear functions over a triangulation of $\widetilde{S}$. The finite element solution τ_h of (9)–(11) is presented in Figure 4 (right).

The actual period of oscillations T is estimated as a weighted average of the exit times over a suitably chosen set (line segment) γ

$$T(\gamma) = \int_\gamma \tau(x, y)\, P_s(x, y)\,\mathrm{d}\gamma \,\Big/ \int_\gamma P_s(x, y)\,\mathrm{d}\gamma. \tag{12}$$

A natural choice of the line segment is $\gamma = \{(x, y) : x = x^f,\ 0 \le y \le y^f\}$, where (x^f, y^f) is the unstable focus of the system $\mathrm{d}x/\mathrm{d}t = v_x$ and $\mathrm{d}y/\mathrm{d}t = v_y$, cf. (3). However, if the line segment γ is slightly shifted to $x = 0.87x^f$ then formula (12) provides more accurate results, as we can observe in Figure 3. The left panel shows the period of oscillations as a function of k_{1d} and the right one as a function of V.

5. Conclusions

To conclude, we stress that the period of oscillation can be computed by (12) using the solution of the Fokker-Planck equation (6) and of the τ-equation (9) with no need of long time stochastic simulations. Figure 3 shows the accuracy of this approach.

The presented technique is not limited to simple system (1)–(2). It can be applied for example to systems with more than two chemical species which are of great interest especially in the cell cycle modeling. This however requires numerical solution of high dimensional Fokker-Planck and τ-equations.

References

[1] R. Erban, J. Chapman, I. Kevrekidis, T. Vejchodský: *Analysis of a stochastic chemical system close to a SNIPER bifurcation of its mean-field model*, submitted to SIAM J. Appl. Math., 2008.

[2] D. Gillespie: *Exact stochastic simulation of coupled chemical reactions.* J. Phys. Chem. **81** (1977), 2340–2361.

[3] J. Tyson, A. Csikasz-Nagy, B. Novak: *The dynamics of cell cycle regulation.* BioEssays **24** (2002), 1095–1109.